

Quantifying Peptides in Isotopically Labeled Protease Digests by Ion Mobility/Time-of-Flight Mass Spectrometry

Jennifer M. Kindy,[†] John A. Taraszka,[†] Fred E. Regnier,[‡] and David E. Clemmer^{*,†}

Department of Chemistry, Indiana University, Bloomington, Indiana 47405, and Department of Chemistry, Purdue University, Lafayette, Indiana 47907

Ion mobility/time-of-flight techniques have been used to analyze mixtures of isotopically labeled peptides. The isotopic labels were generated by treatment of peptides with *N*-acetoxy succinimide (or the deuterated analogue), which results in acetylation (or deuterioacetylation) of the primary amines (i.e., the N-terminus and lysine residues). The relative concentrations of a peptide in each sample are determined by comparing the peak intensities for isotopic pairs. An important consideration is that as mixtures become increasingly complex, isotopic pairs of peaks may overlap with other peaks in the mass spectrum. The influence of the acetyl and deuterioacetyl groups on the mobilities of peptides is considered. The coincidence in mobilities of isotopic pairs provides a means of distinguishing isotopic pairs from other isobaric interferences.

Mass spectrometry (MS) techniques and isotopic labeling strategies have been used extensively for elucidating structures and reaction mechanisms.¹ Recently, approaches aimed at the use of isotopic labels for peptide analysis have been developed. By incorporating an isotopic label that is positioned at specific sites in peptides, it is possible to create what is effectively a mixture of internal standards, one for each component in the sample. Comparison of peak intensities for the heavy and light isotopically labeled species can be used to determine relative abundances of a specific peptide with respect to its internal standard.

Several of these strategies are currently receiving considerable attention. The isotope-coded affinity tag, or ICAT reagent, targets cysteine residues and thus can be used to label cysteine-containing peptides.^{2,3} This approach has recently been used to correlate changes in protein abundance to mRNA levels in yeast² and also to compare protein expression in yeast cells grown in media with ethanol or galactose as the carbon source.³ The reagent includes biotin for selection of cysteine-containing peptides using a streptavidin column. Although this approach simplifies the mixture, peptides that do not contain a cysteine will be missed, limiting the use of this approach for examining posttranslational modifications. Additional cysteine-specific approaches include S-carboxymethylation of the thiol group with ¹³C₂-labeled bromoacetic acid⁴

or alkylation of the side chain with deuterium-enriched acrylamide.⁵

Ji et al. describe an alternative method that involves acetylation (or deuterioacetylation) of primary amines (i.e., the N-terminus and the lysine side chains).^{6,7} This approach is universal for all peptides that contain a primary amino group. The method also provides some sequence information, because the number of acetylations on the peptide serves as an indicator of whether the tryptic peptide contains a lysine or an arginine residue at the C-terminus.

A number of other techniques make use of site-specific isotopic labeling for peptide sequencing by MS/MS. Chen et al. have modified the N-terminus of peptides with 2,4-dinitrofluorobenzene (DNFB) or [²H₃]DNFB for MS/MS sequencing of cross-linked peptides.⁸ Münchbach et al. have reported nicotinylation specific to the N-terminus at pH 5.0 with 1-([⁴H₄]nicotinoyloxy)-succinimide and 1-([⁴D₄]nicotinoyloxy)-succinimide.⁹ Hunt et al. utilized N-terminal acetylation (or deuterioacetylation) to sequence peptides by collision activated dissociation (CAD).¹⁰

Isotopic labeling at the C-terminus can be accomplished by digesting proteins in ¹⁸O-labeled water,^{11–20} resulting in incorporation of ¹⁸O at the C-terminus of tryptic fragments (with the

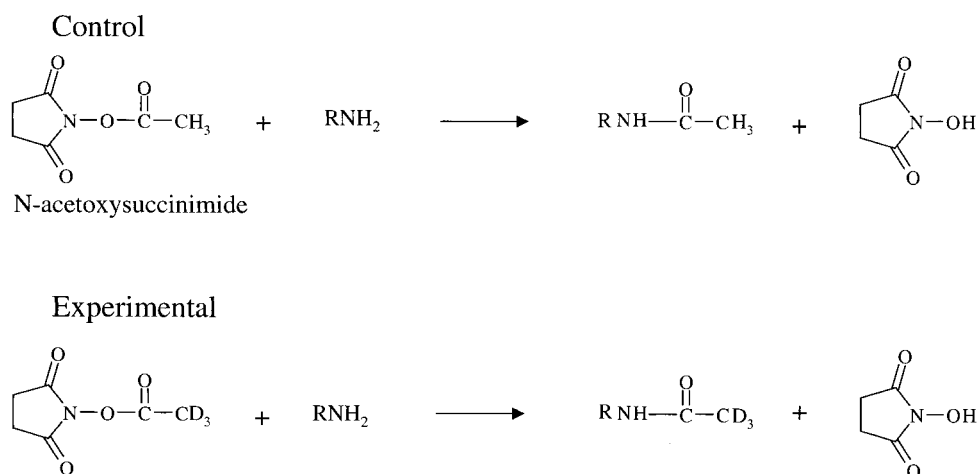
- (4) Adamczyk, M.; Gebler, J. C.; Wu, J. *Rapid Commun. Mass Spectrom.* **1999**, *13*, 1813–1817.
- (5) Sechi, S.; Chait, B. T. *Anal. Chem.* **1998**, *70*, 5150–5158.
- (6) Ji, J.; Chakraborty, A.; Geng, M.; Zhang, X.; Amini, A.; Bina, M.; Regnier, F. *J. Chromatogr. B* **2000**, *745*, 197–210.
- (7) Geng, M.; Ji, J.; Regnier, F. E. *J. Chromatogr. A* **2000**, *870*, 295–313.
- (8) Chen, X. H.; Chen, Y. H.; Anderson, V. E. *Anal. Biochem.* **1999**, *273*, 192–203.
- (9) Münchbach, M.; Quadroni, M.; Miotto, G.; James, P. *Anal. Chem.* **2000**, *72*, 4047–4057.
- (10) Hunt, D. F.; Buko, A. M.; Ballard, J. M.; Shabanowitz, J.; Giordani, A. B. *Biomed. Mass Spectrom.* **1981**, *8*, 397–408.
- (11) Desiderio, D.; Kai, M. *Biomed. Mass Spectrom.* **1983**, *10*, 471–479.
- (12) Rose, K.; Simona, M.; Offord, R.; Prior, C.; Otto, B.; Thatcher, D. *Biochem. J.* **1983**, *215*, 273–277.
- (13) Rose, K.; Savoy, L.-A.; Simona, M. G.; Offord, R. E.; Wingfield, P. *Biochem. J.* **1988**, *250*, 253–259.
- (14) Gaskell, S. J.; Haroldsen, P. E.; Reilly, M. H. *Biomed. Environm. Mass Spectrom.* **1988**, *16*, 31–33.
- (15) Takao, T.; Hori, H.; Okamoto, K.; Harada, A.; Kamachi, M.; Shimonishi, Y. *Rapid Commun. Mass Spectrom.* **1991**, *5*, 312–315.
- (16) Schnolzer, M.; Jedrzejewski, P.; Lehman, W. D. *Electrophoresis* **1996**, *17*, 945–953.
- (17) Shevchenko, A.; Chernushevich, I.; Ens, W.; Standing, K. G.; Thomson, B.; Wilm, M.; Mann, M. *Rapid Commun. Mass Spectrom.* **1997**, *11*, 1015–1024.
- (18) Qin, J.; Herring, C. J.; Zhang, X. *Rapid Commun. Mass Spectrom.* **1998**, *12*, 209–216.
- (19) Kosaka, T.; Takazawa, T.; Nakamura, T. *Anal. Chem.* **2000**, *72*, 1179–1185.

[†] Indiana University.

[‡] Purdue University.

- (1) McLafferty, F. W.; Turecek, F. *Interpretation of Mass Spectra*, 4th ed.; University Science Books: Mill Valley, CA, 1993.
- (2) Ideker, T.; et al. *Science* **2001**, *292*, 929–934.
- (3) Gygi, S. P.; Rist, B.; Gerber, S. A.; Turecek, F.; Gelb, M. H.; Aebersold, R. *Nat. Biotechnol.* **1999**, *17*, 994–999.

Scheme 1



exception of the fragment from the original protein C-terminus). Deglycosylation of undigested proteins in 50% H_2^{18}O was used by Kuster et al. to convert glycosylated asparagine residues to 50% ^{18}O -labeled aspartic acid residues in order to identify glycosylation sites from the resulting mass spectral doublets.²¹ Similarly, phosphorylation sites have been evaluated by incorporation of ethanethiol or ethane- d_5 -thiol upon β -elimination of the phosphate group.²²

A general complication arises for isotopic labeling studies involving very large mixtures. In such complex systems, other species may have mass-to-charge (m/z) ratios that overlap with one or both members of the isotopically labeled pair. Such interferences will preclude accurate abundance measurements. One method for simplifying complex mixtures is to incorporate on-line separation strategies; however, this approach must be used with some caution, because the retention times of isotopic pairs may not be identical.²³ Another approach is to utilize the higher resolving power and mass accuracy associated with Fourier transform mass spectrometry to resolve complex mixtures of isotopically labeled peptides.²⁰ In this paper, we examine the utility of a combined ion mobility-MS approach for analysis of complex mixtures of isotopic pairs of acetylated and deuterioacetylated peptides. In many cases, peaks that cannot be resolved on the basis of differences in m/z can be separated on the basis of differences in their mobilities.²⁴ In the present studies, we find that for all of the peptides that we have examined, heavy and light pairs have mobilities that are identical (within the experimental uncertainty). Thus, the peaks corresponding to heavy and light pairs can be identified on the basis of the coincidence in their drift times, even if other species are present at the same m/z ratio. We demonstrate the approach by examining several mixtures of tryptic peptides.

(20) Yao, X.; Freas, A.; Ramirez, J.; Demirev, P. A.; Feneselau, C. *Anal. Chem.* **2001**, *73*, 2836–2842.

(21) Kuster, B.; Mann, M. *Anal. Chem.* **1999**, *71*, 1431–1440.

(22) Weckwerth, W.; Willmitzer, L.; Fiehn, O. *Rapid Commun. Mass Spectrom.* **2000**, *14*, 1677–1681.

(23) Zhang, R.; Sioma, C. S.; Wang, S.; Regnier, F. E. *Anal. Chem.* **2001**, *73*, 5142–5149.

(24) For a discussion of which types of structural differences can be resolved by the combined IMS-TOF approach, see: Taraszka, J. A.; Counterman, A. E.; Clemmer, D. E. *Fresenius' J. Anal. Chem.* **2001**, *369*, 234–245.

EXPERIMENTAL SECTION

General. Experiments were carried out using a home-built high-resolution ion mobility/time-of-flight (TOF) mass spectrometer that is described elsewhere;^{25,26} only a brief description is presented here. Ions are generated by electrospray ionization of a $1.0 \text{ mg}\cdot\text{mL}^{-1}$ solution of total tryptic digest in 49:49:2 (% volume) water/acetonitrile/acetic acid under ambient laboratory conditions. The ions are directed through a capillary into a differentially pumped region at the front of the drift region. A $300\text{-}\mu\text{s}$ pulse of ions is gated into the 52.8-cm-long drift region that is operated at a pressure of ~ 152 Torr He and a field strength of $151.5 \text{ V}\cdot\text{cm}^{-1}$. While in the drift tube, the ions are separated on the basis of differences in their mobilities through the buffer gas. The mobilities depend on the ions' charge states and collision cross sections. Highly charged ions experience a stronger drift force (zeV) than lower charge state ions and, therefore, have higher drift velocities. Elongated structures undergo more collisions with the buffer gas and, therefore, have lower drift velocities than more compact structures.

At the back of the drift tube, high-voltage pulses ($1.0 \mu\text{s}$) direct ions into an orthogonal geometry reflectron TOF instrument. Measurements of flight times in the mass spectrometer are used to determine m/z ratios. Because drift times are on the order of milliseconds and flight times are on the order of microseconds, hundreds of flight time measurements can be acquired across the drift time distribution. We refer to this as a “nested” drift (flight) time measurement, reported as $t_d(t_f)$ with units of $\text{ms}(\mu\text{s})$.

Collision Cross Sections. It is useful to derive experimental collision cross sections. After a small correction to the experimental drift time to account for the time required to travel between the drift tube and the TOF source, the collision cross section is derived from the experimental measurement from the relation²⁷

$$\Omega = \frac{(18\pi)^{1/2}}{16} \frac{ze}{(k_b T)^{1/2}} \left[\frac{1}{m_1} + \frac{1}{m_b} \right]^{1/2} \frac{t_d E_D}{L P} \frac{760}{273.2 N} \quad (1)$$

where ze corresponds to the charge of the ion; m_1 and m_b are the

(25) Srebalus, C. A.; Li, J.; Marshall, W. S.; Clemmer, D. E. *Anal. Chem.* **1999**, *71*, 3918–3927.

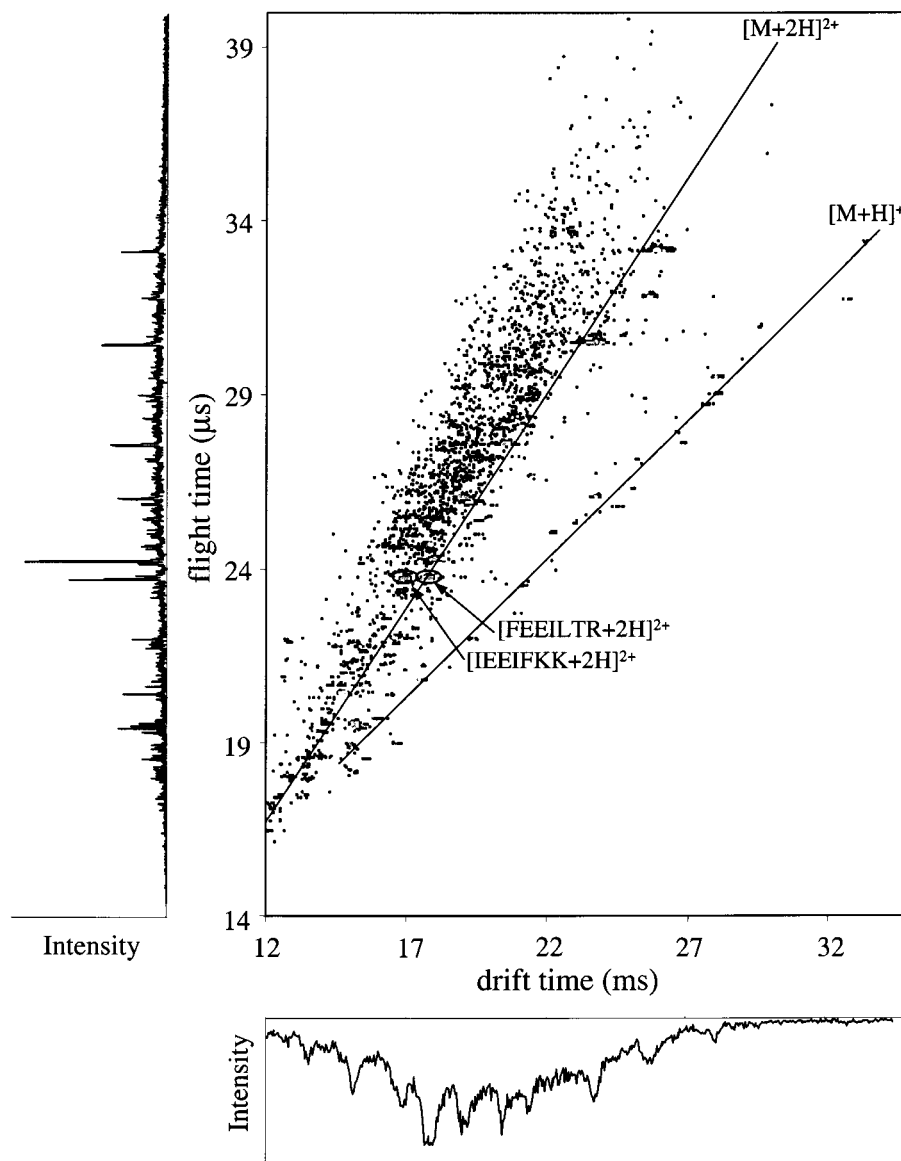


Figure 1. Contour plot of nested drift (flight) times for an unlabeled creatine phosphokinase (rabbit) tryptic digest. The lines drawn on the plot indicate the locations of the $[M + H]^+$ and $[M + 2H]^{2+}$ families. The mass spectrum at the left was obtained by summing all intensities at each flight time across the drift time distribution. The drift time spectrum at the bottom was obtained by integration across the flight region for each drift time. Data are shown using a baseline cutoff of 2.

masses of the ion and the buffer gas, respectively; P is the pressure of the buffer gas in the drift tube; T is the temperature of the buffer gas; t_D is the drift time; E is the electric field strength; L is the length of the drift tube; N is the number density of neutrals present; and k_b is Boltzmann's constant.

Synthesis of *N*-Acetoxy- d_3 -succinimide and *N*-Acetoxy-succinimide. *N*-hydroxysuccinimide (Sigma), acetic anhydride (>99% purity, Aldrich), and acetic anhydride- d_6 (>99% purity, Aldrich) were used as received. *N*-acetoxy succinimide and its d_3 -analogue were synthesized by a procedure that is similar to a method published previously.⁶

Tryptic Digestion of Proteins. Albumin (bovine), creatine phosphokinase (rabbit), enolase (yeast), hemoglobin (pigeon), and

trypsin (TPCK-treated bovine pancreas) were purchased from Sigma and used as received. Proteins were dissolved in a 0.2 M ammonium bicarbonate (EM Science) solution and digested by addition of 150 μ L of a 5.0 mg·mL⁻¹ trypsin solution in 0.2 M ammonium bicarbonate. The digest was incubated for ~20 h at 37 °C, and the trypsin was removed by filtration using a microconcentrator (microcon 10, Amicon). The resulting peptides were lyophilized.

Generation of Acetylated and Deuterioacetylated Tryptic Peptide Mixtures. Acetylated and deuterioacetylated peptides were generated as described previously.⁶ A brief summary is given here; the reactions (where R represents any tryptic peptide) used to produce acetylated and deuterioacetylated peptide mixtures are shown in Scheme 1.

An excess of *N*-acetoxy succinimide (or the d_3 -analogue) was added to solutions (1 mg·mL⁻¹) of tryptic peptides in a phosphate

(26) Hoaglund, C. S.; Valentine, S. J.; Sporleder, C. R.; Reilly, J. P.; Clemmer, D. E. *Anal. Chem.* **1998**, *70*, 2236–2242.

(27) Mason, E. A.; McDaniel, E. W. *Transport Properties of Ions in Gases*; Wiley: New York, 1988.

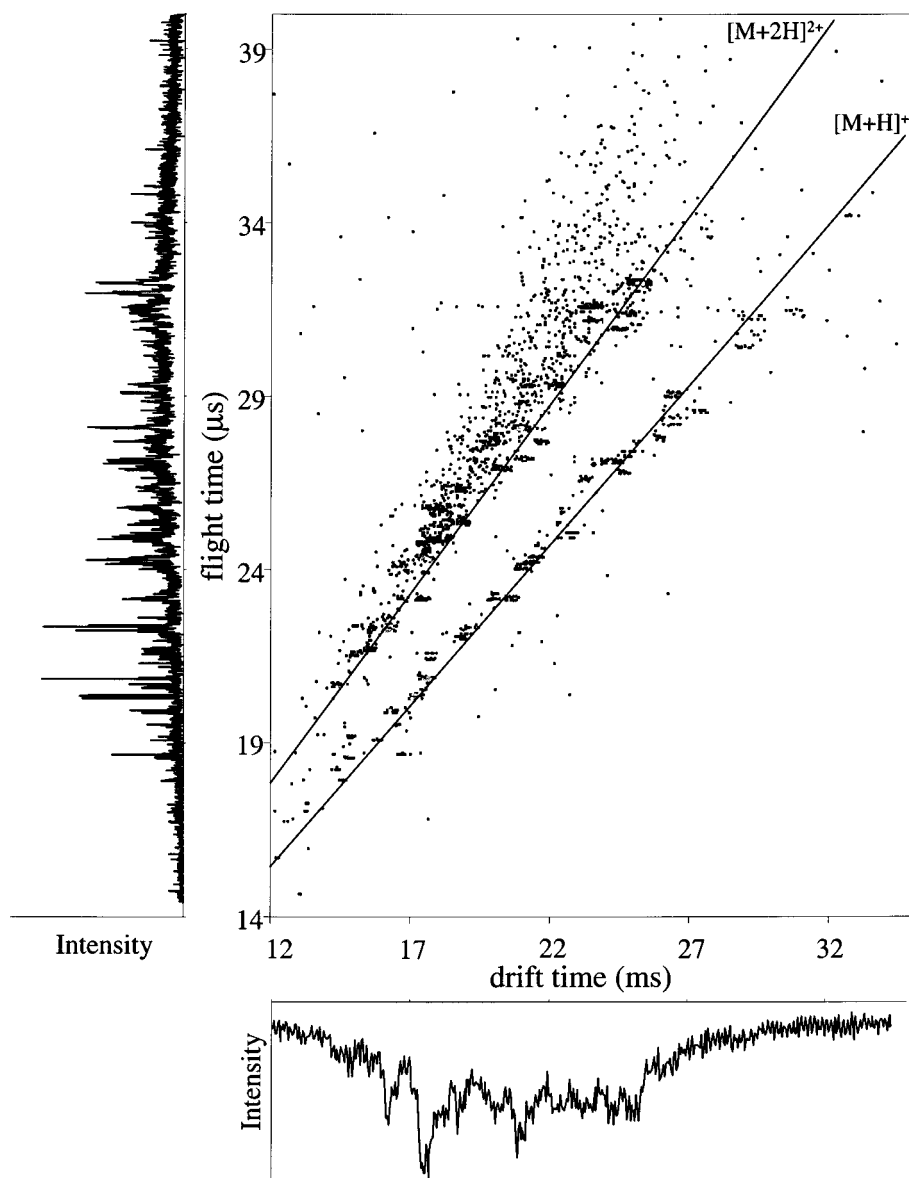


Figure 2. Two-dimensional plot of a nested $t_d(t)$ dataset for a 1:1 mixture of acetylated and deuterioacetylated creatine phosphokinase tryptic peptides. Data are shown using a baseline cutoff of 2. Summed mass (left) and drift (bottom) spectra were obtained as described in Figure 1.

buffer of pH 7.5. After stirring for 5 h, equal aliquots of each solution were combined and purified on a semipreparatory scale C_{18} column (250×21.2 mm) from Vydac using high-performance liquid chromatography (HPLC) (Waters, model 600). Deionized water and acetonitrile (Fisher, Optima grade), each with 0.1% trifluoroacetic acid were used as the mobile phases. It is possible that some peptides, especially those in very small quantities, may be lost during this step; however, we note that we expect any discrimination to influence the light and heavy-labeled peptides in the same ways. The resulting mixture of acetylated and deuterioacetylated peptides was dried by rotary evaporation and lyophilized.

RESULTS AND DISCUSSION

Nested Drift (Flight) Time Distribution for an Unlabeled Digest. It is useful to begin by examining a typical nested $t_d(t)$ dataset for a mixture of tryptic peptides. Figure 1 shows a two-dimensional dataset recorded for tryptic peptides of creatine

phosphokinase (rabbit). This dataset is similar to many other datasets that we have recorded for similar samples. The 14.0–40.0- μ s flight time range that is shown corresponds to the range $m/z = 154.9$ –1306.2. As discussed previously,²⁸ peaks fall into $[M + H]^+$ and $[M + 2H]^{2+}$ charge state families. At a given flight time, the variability in drift times across a single charge state is ~ 20 –25%.²⁴ A comparison of the two-dimensional plot with the integrated mass spectrum (also shown) reveals that many broad (or unresolved) peaks in the mass spectrum can be resolved into multiple sharp peaks in the two-dimensional dataset. For example, a partially resolved doublet at 23.725 and 23.735 μ s (in the mass spectrum) corresponds to peaks for the $[FEEILTR + 2H]^{2+}$ (m/z 454.4) and $[IEEIFKK + 2H]^{2+}$ (m/z 454.0) ions that are clearly separated in the two-dimensional dataset. Overall, we are able to assign 32 peaks to 28 tryptic or chymotryptic fragments (four are

(28) Valentine, S. J.; Counterman, A. E.; Hoaglund, C. S.; Reilly, J. P.; Clemmer, D. E. *J. Am. Soc. Mass Spectrom.* **1998**, *9*, 1213–1216.

Table 1. Peptides Identified in the Unlabeled and Isotopically Labeled Creatine Phosphokinase Digest^a

| peptide sequence ^b | identified in unlabeled mixture | | | identified in labeled mixture | | |
|-------------------------------|---------------------------------|-------------------------------|------------------------------|-------------------------------|-------------------------------|------------------------------|
| | charge ^c | exptl ^d <i>m/z</i> | calc ^e <i>m/z</i> | charge ^c | exptl ^d <i>m/z</i> | calc ^e <i>m/z</i> |
| GERR | 2+ | 259.2 | 259.1 | | | |
| LNYK | 2+, 1+ | 269.1, 537.6 | 269.2, 537.3 | | | |
| VR | 1+ | 274.4 | 274.2 | 1+ | 316.3, 319.4 | 316.3, 319.2 |
| EVFR | 2+, 1+ | 275.7, 550.5 | 275.7, 550.3 | 1+ | 592.7, 595.4 | 592.3, 595.3 |
| HK | 1+ | 284.3 | 284.2 | 1+ | 368.3, 374.3 | 368.2, 374.2 |
| LR | 1+ | 288.4 | 288.2 | 1+ | 330.2, 333.2 | 330.2, 333.2 |
| GGVHVK | 2+ | 298.9 | 298.7 | 2+, 1+ | 340.7, 343.7; 680.5, 686.4 | 340.7, 343.7; 680.4, 686.4 |
| YK | 1+ | 310.3 | 310.2 | | | |
| TGR | 1+ | 333.4 | 333.2 | | | |
| LAHLSK | 2+, 1+ | 334.9, 668.8 | 334.7, 668.4 | 2+, 2+ | 377.0, 379.8; 397.8; 402.5 | 376.7, 379.7; 397.7; 402.2 |
| YYPLK | 2+, 1+ | 342.4, 683.7 | 342.2, 683.4 | (2ac, 3ac) ^f | | |
| SIK | 1+ | 347.5 | 347.3 | 1+, 1+ | 389.5, 392.5; 431.3, 437.4 | 389.2, 392.2; 431.2, 437.2 |
| DWPDAR | 2+ | 380.4 | 380.2 | (1ac, 2ac) ^f | | |
| HPK | | | | 1+ | 465.3, 471.4 | 465.2, 471.2 |
| LQK | 1+ | 388.4 | 388.3 | 1+ | 472.4, 478.4 | 472.3, 478.3 |
| IEEIFK | 2+ | 390.0 | 389.7 | | | |
| GKYYPLK | 2+ | 435.0 | 434.8 | | | |
| LMVEMEK | 2+ | 440.3 | 440.2 | | | |
| AVEK | 1+ | 446.5 | 446.3 | | | |
| IEEIFKK | 2+ | 454.0 | 453.8 | | | |
| FEEILTR | 2+ | 454.4 | 454.2 | 2+ | 475.4, 477.0 | 475.2, 476.7 |
| KLR | | | | 1+ | 500.5, 506.5 | 500.3, 506.3 |
| VRTGRSIK | 2+ | 458.3 | 458.8 | | | |
| VLTPDLYK | 2+ | 475.0 | 474.8 | 2+ | 517.0, 519.9 | 516.8, 519.8 |
| GIWHNDNK | 2+ | 492.7 | 492.2 | 2+ | 534.3, 537.3 | 534.2, 537.2 |
| GGNMK | 1+ | 506.5 | 506.2 | | | |
| HGGFKPTDK | | | | 2+ | 556.9, 561.4 | 556.8, 561.3 |
| AGHPF | | | | 1+ | 570.5, 573.6 | 570.3, 573.3 |
| TDLNHENLK | 2+ | 542.6 | 542.3 | 2+ | 584.5, 587.4 | 584.3, 587.3 |
| FSEVLKRLR | 2+ | 574.5 | 574.4 | | | |
| SEEEYPDLK | 2+ | 599.0 | 598.8 | | | |
| DLFDPIIQDR | | | | 2+ | 637.4, 639.1 | 637.3, 638.8 |
| VLTPEMDAELR | 2+ | 637.6 | 637.3 | | | |
| SFLVWVNEEDHLR | | | | 2+ | 844.0, 845.5 | 843.4, 844.9 |

^a Peptides identified in Figure 1 for the unlabeled mixture and in Figure 2 for the labeled mixture. ^b Expected peptide sequences were predicted from <http://ca.expasy.org/tools/peptide-mass.html>. ^c Charge of the ion(s) assigned to the peptide sequence. ^d Experimental *m/z* ratios were calculated from measured flight times (*t_f*) using a calibration determined from a TOF spectrum of bradykinin. When two *m/z* ratios are given, they correspond to the two different charge states listed in the previous column. Uncertainties in *m/z* ratios are approximately ± 0.5 u. ^e Calculated *m/z* ratios correspond to the monoisotopic peak of the peptide in the charge state(s) listed. When two *m/z* ratios are given, they correspond to the two different charge states listed in the charge column. ^f Peptide sequences LAHLSK and SIK were assigned to the peak pairs in the same charge state family but with a different number of acetylations. The number of acetylations for the two pairs are listed in parentheses under the charge states of the two sequences.

observed as both 1+ and 2+ ions) of creatine phosphokinase, representing ~23% of the total protein sequence.

Nested Drift (Flight) Time Data for Pairs of Light and Heavy Isotopically Labeled Peptides. Figure 2 shows a nested *t_f*(*t*) distribution recorded for an isotopically labeled tryptic peptide mixture of the creatine phosphokinase protein. This spectrum is similar in appearance to the data shown in Figure 1. Peaks fall into [M + H]⁺ and [M + 2H]²⁺ charge state families; however, the distribution of peaks has shifted such that more peptides appear as [M + H]⁺ ions, and fewer are observed as [M + 2H]²⁺. Careful inspection of this dataset reveals that nearly every feature is a doublet. As expected, doublet peaks are separated by three, six, or nine mass units, indicating that one, two, or three acetyl groups have been incorporated by each peptide. We are able to assign 21 of these doublets to labeled forms of 18 expected tryptic peptides (1 is seen in two charge states, 2 are seen with different degrees of acetylation). The 18 labeled peptides represent ~15% of the total protein sequence.

The experimental data and assignments are summarized in Table 1, along with the peptides identified in the unlabeled digest. We note that 16 peptides were observed in the unlabeled mixture

but not in the isotopically labeled mixture; 6 were observed in the isotopically labeled mixture but not in the unlabeled mixture. Overall, the differences between the observations for labeled and unlabeled mixtures can be understood by considering the influence of the label on the expected sites of protonation. The most basic sites in many unlabeled peptides (e.g. the amino terminus and Lys side chain) may be blocked upon acetylation. Thus, we expect the distribution of ions to shift to lower charge states; it is possible that ionization of some peptides is suppressed altogether upon labeling.

Figure 3 shows a plot of a narrow *m/z* range (*m/z* = 530–630) of this dataset. Peaks for the isotopically labeled pairs have very similar drift times, regardless of the number of acetyl groups that have been added to the peptide. For example, the maximum peak intensities for the light and heavy pair of peaks for triply acetylated [Ac₃-HGGFKPTDK + 2H]²⁺ are found at 18.81 ms and 18.82 ms. The ~0.05% shift is about the same as that found for the centers of the peaks for singly acetylated [Ac-EVFR + H]⁺ ions (24.26 and 24.24 ms, or 0.08%).

Figure 3 also shows several simplified mass spectra obtained by integrating across drift time regions that correspond to

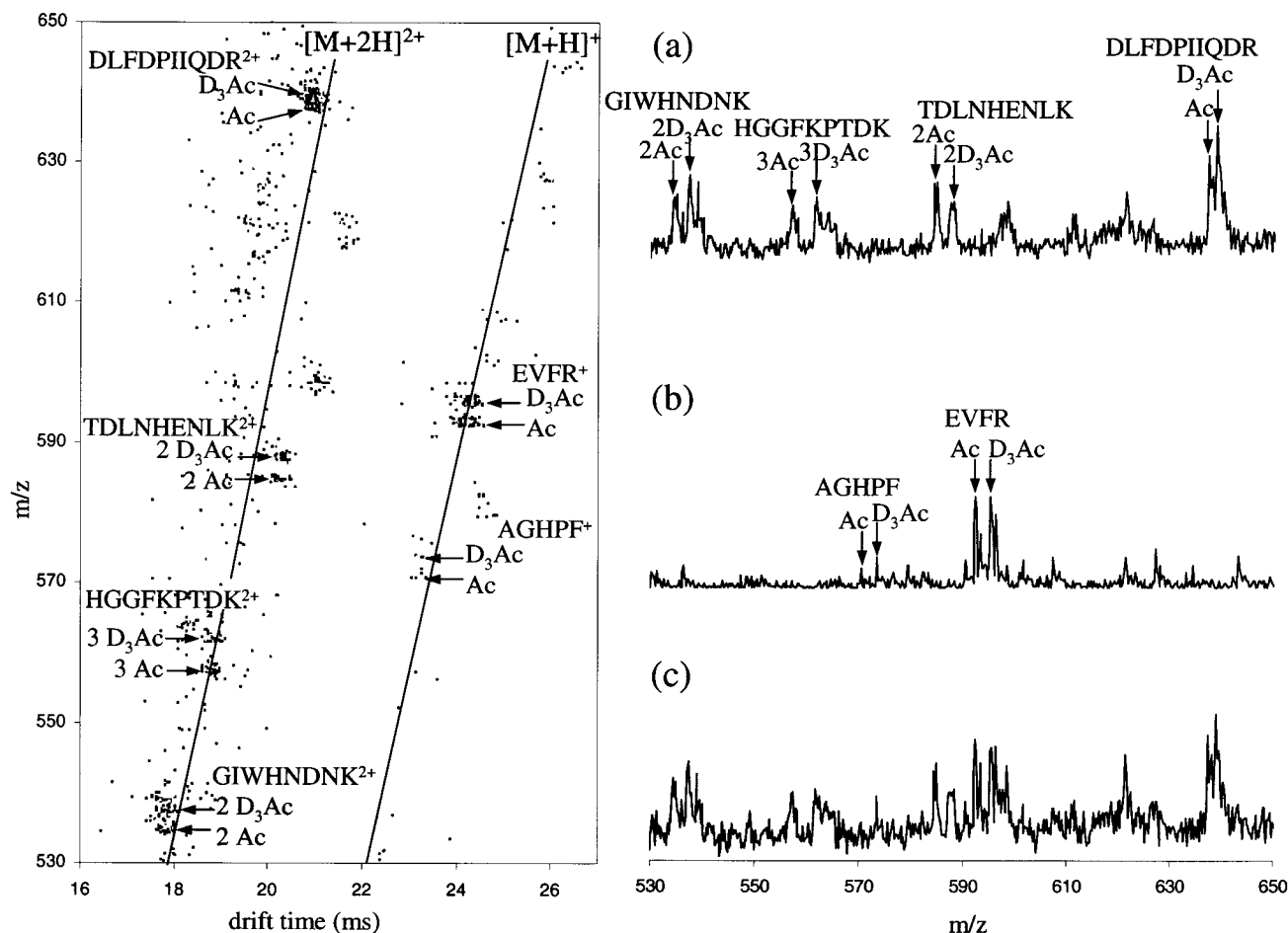


Figure 3. Expanded region of the contour plot from Figure 2 with peaks identified as acetylated and deuteroacetylated peptide pairs indicated on the plot. Ac signifies an acetylated peak and D₃Ac signifies a deuteroacetylated peak, with the leading number indicating the number of acetyl groups on the peptide (those with no number have one acetyl group). Mass spectra were obtained by integration across the appropriate drift time region for: (a) the 2+ charge state family, (b) the 1+ charge state family, or (c) across all drift times to include all ions.

individual charge state families. This approach reduces spectral congestion, and because the charge state is known, the mass shift and, thus, the number of acetyl groups is unambiguous. Shifts of 3 or 6 (and occasionally 9) m/z units are expected for pairs in the $[M+H]^+$ family; shifts of 1.5 or 3 (and occasionally 4.5) are expected for pairs in the $[M+2H]^{2+}$ family. The reduction in spectral congestion simplifies measurements of peak intensities for each isotopic pair. From these integrated mass spectra it is straightforward to determine the relative abundances of the light and heavy labeled pairs. The relative intensities of the acetylated and deuteroacetylated peak pairs shown in Figure 3 are 1.0:1.3 [Ac_2 -GIWHNDNK + 2H]²⁺, 1.0:1.2 [Ac_3 -HGGFKPTDK + 2H]²⁺, 1.0:1.2 [Ac-AGHPF + H]⁺, 1.0:0.97 [Ac_2 -TDLNHENLK + 2H]²⁺, 1.0:1.0 [Ac-EVFR + H]⁺, and 1.0:1.3 [Ac-DLFDPIIQDR + 2H]²⁺.

Using the Coincidence in Drift Times to Identify Isotopic Pairs in Complex Samples. To further illustrate this approach we have examined spectra of more complex mixtures. Data for isotopically labeled tryptic digests of bovine albumin, rabbit creatine phosphokinase, yeast enolase, and pigeon hemoglobin were acquired sequentially into the single nested $t_d(t)$ distribution shown in Figure 4. Peaks in the dataset containing peptides from all four proteins are assigned by comparison with the data recorded for the digests individually. The complexity of this sample is such that many features in the integrated mass spectrum

fall on top of a significant baseline signal; however, many features are resolved in the $t_d(t)$ two-dimensional plot. Overall, a total of 95 peak pairs were assigned to tryptic or chymotryptic peptides expected from these four proteins.

A more detailed view of a smaller region of the $t_d(t)$ dataset is shown in Figure 5. In this region of the spectrum, many peaks that are completely lost in the summed mass spectrum can be resolved in the two-dimensional dataset. For example, the peak corresponding to doubly deuteroacetylated [$(D_3Ac)_2$ -DTHK + H]⁺ (designated a25–28 on the plot) at $m/z = 590.3$ cannot be observed in the integrated mass spectrum (for all ions) because of the large peak associated with the deuteroacetylated [D_3Ac -VASLR + H]⁺ (a101–105) at $m/z = 590.5$. Additionally, the peak for doubly acetylated [Ac_2 -DTHK + H]⁺ at $m/z = 584.3$ appears as a shoulder on the peak for triply deuteroacetylated [$(D_3Ac)_3$ -KYH + H]⁺ (hb144–146) at $m/z = 582.2$. However, incorporation of the mobility separation allows all species for the three peptides to be separated.

It is instructive to discuss several other examples that illustrate the advantage of the mobility separation shown in Figure 5. For example, two pairs of low-intensity peaks that would appear on top of each other in a summed mass spectrum correspond to [Ac_3 -HGGFKPTDK + 2H]²⁺ (cm97–105) at $m/z = 556.9$ and 561.4 and [Ac_3 -VHWSAEEK + 2H]²⁺ (ha1–8) at $m/z = 556.5$ and 561.1.

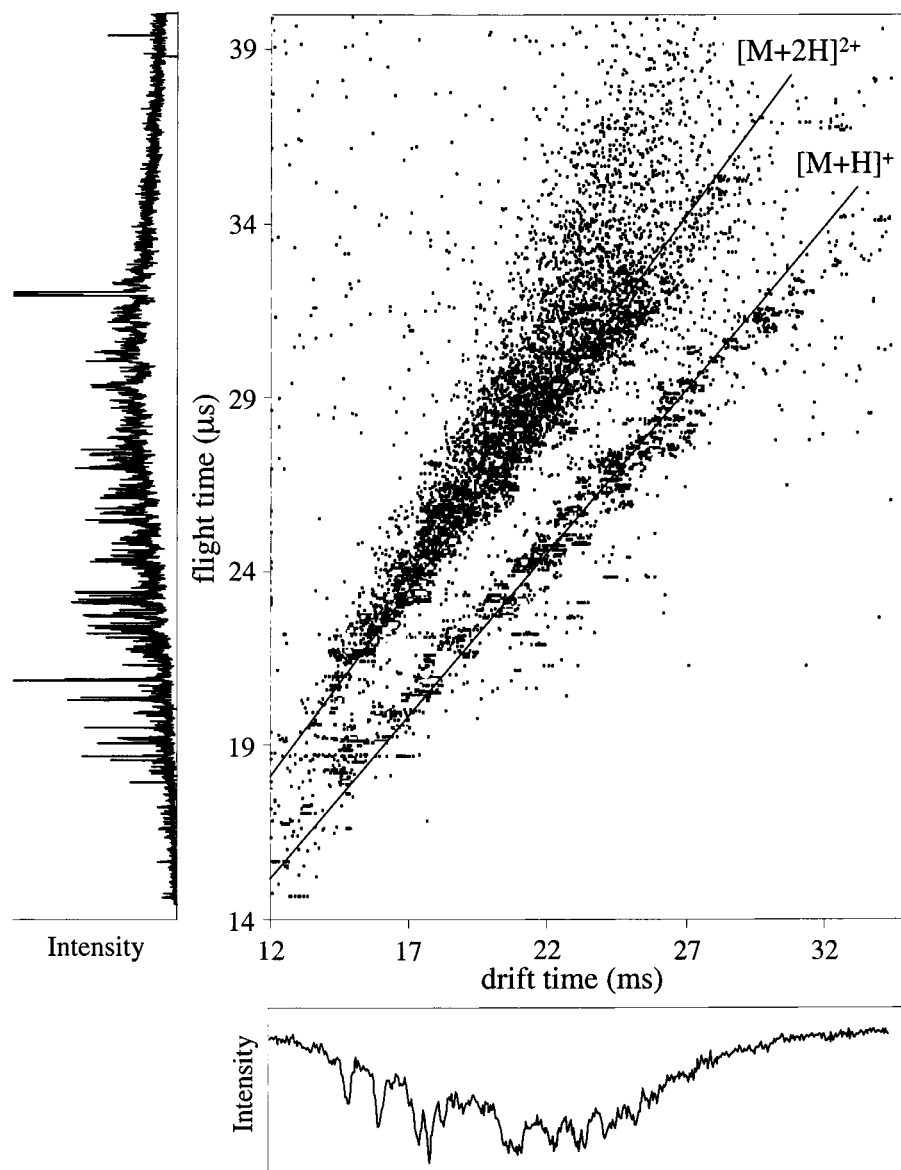


Figure 4. Contour plot consisting of combined nested $t_d(t)$ datasets for acetylated and deuterioacetylated peptides from tryptic digests of bovine albumin, rabbit creatine phosphokinase, yeast enolase, and pigeon hemoglobin. The data are shown using a baseline cutoff of 2.

In this case, assignments can be made only on the basis of comparison of mobilities with data for individual digests. An additional example is associated with the peaks for $[\text{Ac-VYAR} + \text{H}]^+$ and $[\text{D}_3\text{Ac-VYAR} + \text{H}]^+$ (e5–8) at $m/z = 550.5$ and 553.5 . This pair of peaks is found at a slightly shorter drift time than the more intense peaks for $[\text{Ac-FGER} + \text{H}]^+$ and $[\text{D}_3\text{Ac-FGER} + \text{H}]^+$ (a229–232) at $m/z = 550.2$ and 553.5 . Similarly, the low-intensity peaks for $[\text{Ac-LVVSTQ} + \text{H}]^+$ (a598–607) at $m/z = 523.0$ and 524.5 are separated from the deuterioacetylated peak of $[\text{Ac}_3\text{-LSDLHAQK} + \text{H}]^+$ (ha83–90) at $m/z = 523.8$ by a small difference in drift time. Several other examples of the utility of the mobility separation in aiding to resolve peaks that have nearly identical m/z ratios can be observed by inspection of Figure 5.

Finally, we note that the reduction in spectral congestion associated with the mobility separation translates into a more accurate determination of relative intensities of isotopically labeled pairs. A summary of relative ratios of acetylated and deuterioacetylated peptides for all of the peaks that were analyzed for

tryptic fragments from the four different proteins is provided in Table 2.

Variability in Unlabeled/Acetylated and Acetylated/Deuterioacetylated Peptide Ion Cross Sections. It is instructive to consider the variability in cross sections (or mobilities) associated with the unlabeled and labeled peptides and also with acetylated and deuterioacetylated peptides. The former comparison provides insight about the effect of acetylation on ion structure. The latter illustrates the degree to which the mobility coincidence can be used as a means of identifying light and heavy ion pairs.

Figure 6 shows a plot of the ratio of acetylated to unlabeled peptide cross sections (reported previously).²⁹ These results show that incorporation of a single acetyl group results in a cross section increase of ~25–35%. Incorporation of two acetyl groups results in an even larger change. These increases (especially for large

(29) Valentine, S. J.; Counterman, A. E.; Clemmer, D. E. *J. Am. Soc. Mass Spectrom.* **1999**, *10*, 1188–1211.

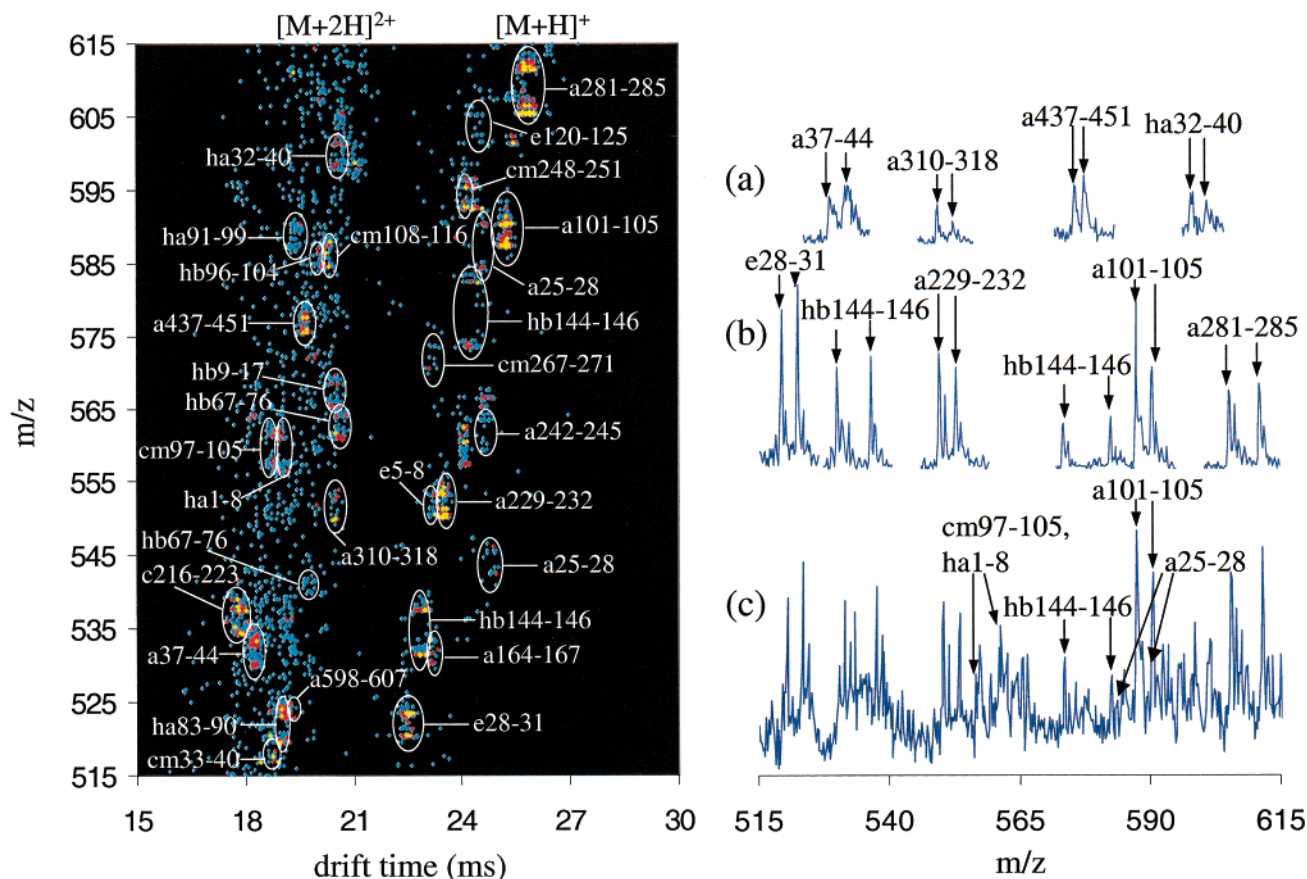


Figure 5. Two-dimensional dataset of the four acetylated and deuterioacetylated digests displayed over the region of m/z 515–615 (~ 25.24 – $27.55 \mu\text{s}$ flight time). The white ovals indicate the locations of peaks assigned to isotopically labeled peptide pairs. The ovals are labeled with a letter indicating the parent protein (a for bovine albumin; c for rabbit creatine phosphokinase, both chains; cm for rabbit creatine phosphokinase, m chain; e for yeast enolase; ha for pigeon hemoglobin, α chain; hb for pigeon hemoglobin, β chain) and a number range indicating the position of the peptide in the primary amino acid sequence of the protein. Integration across a narrow drift range for selected peptide pairs yielded the collection of mass spectra shown at the right for (a) selected 2+ and 3+ ions or (b) selected 1+ ions. A mass spectrum corresponding to integration across all drift time windows is shown in part c.

Table 2. Proteins Included in the Mixture of Four Labeled Digests^a

| protein ^a | ratio of CH ₃ CO:CD ₃ CO peptides in mixture ^b | ratio of CH ₃ CO:CD ₃ CO peptides calcd from intensities in data set ^c | no. peptides identified in mixture ^d |
|---------------------------------|---|---|---|
| albumin (bovine) | 1.0:1.0 | (1.0:0.99) \pm 0.25 | 25 |
| creatine phosphokinase (rabbit) | 1.0:1.0 | (1.0:1.10) \pm 0.21 | 16 |
| enolase (yeast) | 1.0:1.0 | (1.0:1.12) \pm 0.24 | 18 |
| hemoglobin (pigeon) | 1.0:0.98 | (1.0:0.92) \pm 0.16 | 17 |

^a Each protein was digested by trypsin in solution and then acetylated or deuterioacetylated as described in the experimental section. ^b Theoretical ratio of peptides mixed while still in the phosphate buffer solution prior to desalting by HPLC. ^c Ratio was calculated by integration across the drift time distribution for each individual peak to obtain the summed mass spectrum. The concentration ratio for each peptide was calculated by direct comparison of the intensity of the monoisotopic peak for the acetylated and deuterioacetylated species, and then the ratios for all peptides from a given parent were averaged together to obtain the reported ratio. ^d Number of acetylated/deuterioacetylated pairs identified in Figure 4 (within ± 0.5 of the expected m/z) that are unique to the protein.

peptides) are much greater than are expected from the increase associated with the size of the acetyl group. In fact, it appears that acetylation has a rather drastic effect on the overall structure of the peptide ion. Previous work has shown that blocking the N-terminus of polyaniline peptides results in conformations that are substantially more extended.³⁰ In the unblocked polyaniline peptides, presumably protons are associated with the most basic site, the N-terminal amino group. Protonation of this site results

in compact structures in which the protonation site is self-solvated by the polypeptide chain (mostly by electronegative carbonyl groups).³¹ When the proton can associate along the C-terminal side of the peptide, the system can form a stable helix, a much more extended state.^{32,33} Our preliminary analysis of this system suggests that a similar phenomenon can occur in tryptic peptides. We are currently using molecular modeling methods to investigate this in detail.

(30) Kinnear, B. S.; Jarrold, M. F. Personal communication.

(31) Hudgins, R. R.; Mao, Y.; Ratner, M. A.; Jarrold, M. F. *Biophys. J.* **1999**, *76*, 1591–1597.

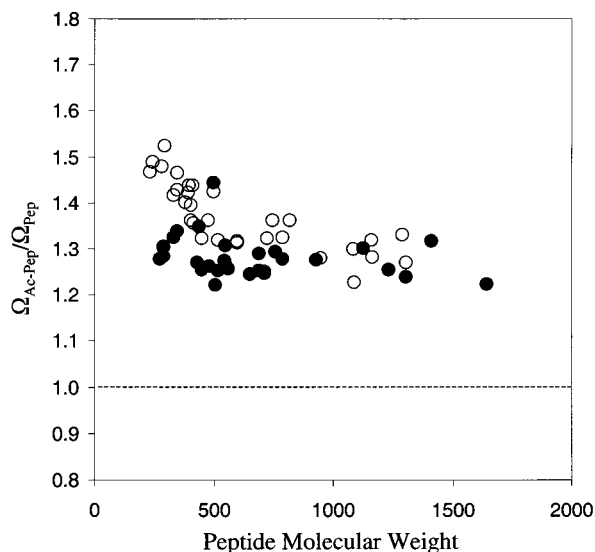


Figure 6. Ratio of cross sections for unlabeled and acetylated peptides plotted as a function of the mass of the unlabeled peptide. The data for the acetylated peptides are taken from the four tryptic digests individually and are all combined on this plot; the cross sections for the unlabeled peptides were taken from ref 29. Peptides that were doubly acetylated are indicated by (\circ); peptides that were singly acetylated are indicated by (\bullet).

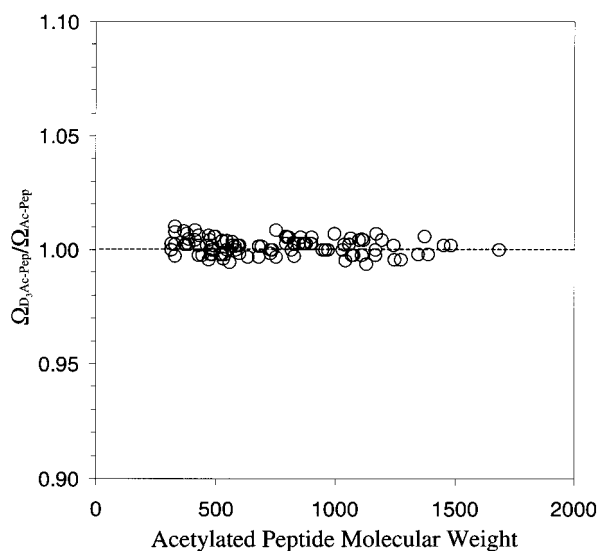


Figure 7. The ratio of the cross section of a deuterioacetylated peptide to the cross section of the acetylated peptide is plotted as a function of the mass of the acetylated peptide. The cross sections were determined from the data shown in Figure 4.

Figure 7 shows a plot of the ratio of cross sections for acetylated and deuterioacetylated peptides that have been determined in this study. In every case that we have examined, peptide cross sections for acetylated and deuterioacetylated peptides differ by less than 0.9%, near the expected relative uncertainty for the experimental measurement. Thus, it appears that deuteration of the label does not affect the structure (or mobility) of these ions. Although we expected this to be the case, it is important to

(32) Hudgins, R. R.; Ratner, M. A.; Jarrold, M. F. *J. Am. Chem. Soc.* **1998**, *120*, 12974–12975.

(33) Counterman, A. E.; Clemmer, D. E. *J. Am. Chem. Soc.* **2001**, *123*, 1490–1498.

demonstrate this, because the coincidence can be combined with the m/z shifts to identify peptide pairs (as discussed above). We note that this may be an important analytical advantage when compared with HPLC/MS approaches, as it appears that retention times for heavy and light pairs of this and other labels do exhibit some variability.²³

SUMMARY AND CONCLUSIONS

We have examined the use of hybrid ion mobility-MS techniques for the analysis of tryptic peptide mixtures that were acetylated (or deuterioacetylated) at primary amines, that is, the N-terminus and lysine side chains. Analysis of an unlabeled creatine phosphokinase (rabbit) tryptic digest resulted in assignment of 28 peptides in the nested $t_d(t)$ dataset; 18 peptides were identified in the dataset for the isotopically labeled mixture of the same digest. The approach was extended to a more complicated system of peptides from four proteins, and 95 peak pairs could be identified.

A benefit of the mobility separations is associated with increased peak capacity compared with mass analysis alone. Peptides that ordinarily overlap in m/z ratio can be resolved in the two-dimensional dataset. We find a coincidence in drift time of the heavy and light isotopically labeled peptides. In all cases, cross sections for isotopic pairs differ by less than 0.9%. This provides an effective method for constraining peak pairs in complex samples. The separation of ions into charge state families also is useful in assigning data. The number of acetylations can be unambiguously determined from the m/z difference between two peaks and the charge of the ions. Although we have focused our discussion on the advantages of the IM-TOF approach, as compared with TOF analysis alone, we note that the time scale of the combined separation is suitable for a three-dimensional approach, LC/IM-TOF. In this case, if there are shifts in the retention times of isotopic pairs of peaks during the LC separation, the identical drift times would provide an additional handle for identifying pairs of peaks. We recently demonstrated that the addition of IMS to an LC-MS can help resolve sequence isomers in peptide libraries.³⁴

Finally, we noted that the acetyl group appears to affect the overall structure of the peptide such that more extended structures are favored.

ACKNOWLEDGMENT

This work was supported by grants from the NIH (1R01GM-59145-01A1). J.M.K. thanks the National Science Foundation for a graduate research fellowship.

Received for review July 18, 2001. Accepted December 13, 2001.

AC010807P

(34) Srebalus-Barnes, C. A.; Hilderbrand, A. E.; Valentine, S. J.; Clemmer, D. E. *Anal. Chem.* **2002**, *74*, 26–36.